Insights in the two-step synthesis of single crystalline Ag2Te nanorods

Karen Al Hokayem, Jaafar Ghanbaja, S. Michel, Sophie Legeai, Nicolas Stein

Insights in the two-step synthesis of single crystalline Ag_2Te nanorods

Karen Al Hokayem[a*], Jaafar Ghanbaja[b], Stéphanie Michel[a], Sophie Legeai[a], Nicolas Stein[a]

[a] *Université de Lorraine, CNRS, IJL, F-57000 Metz, France.*
[b] *Université de Lorraine, CNRS, IJL, F-54000 Nancy, France.*

ARTICLE INFO

Keywords:
Tellurium
Ag_2Te
Nanorods
Chemical synthesis
Single crystalline

ABSTRACT

Pure monoclinic single crystalline Ag_2Te nanorods were synthesized by a two-step method. The first step concerns the electrodeposition of self-standing Te nanorods in an ionic liquid medium, taking advantage of its templating properties. These obtained nanorods are single crystalline with growth direction along the [001] axis in the hexagonal lattice. The average diameter of the as-deposited Te nanorods is 60 ± 13 nm with less than 300 nm long. Afterwards, the resulting nanostructured Te film is immerged in a dedicated silver-based bath in order to be transformed into Ag_2Te binary compounds by a combined mechanism of chemical cementation and topotactic transformation. The chemical analysis reveals that the final nanostructures exhibit a slight excess of silver and TEM-SAED analysis shows that they are still single crystalline with an increase of the initial diameter, less than 30%. HR-TEM highlights the presence of an intermediate stützite phase and the hessite phase α-Ag_2Te is obtained at the end of the synthesis process.

1. Introduction

Silver tellurides (AgTe, Ag_2Te, Ag_5Te_3 and Ag_7Te_4…) are semi-conducting compounds that can be used in data storage devices [1], optical materials [2] and magnetic measurements [3]. Like numerous metal tellurides (PbTe, Bi_2Te_3, $Cu_{1.75}Te$…), Ag_2Te is of high interest as thermoelectric material, converting heat into electricity and vice versa [4]. In the current energy crisis context, thermoelectricity appears as a promising renewable energy route to collect heat waste thus minimizing energy losses. The best thermoelectric materials are characterized by a low thermal conductivity associated with a maximum electrical conductivity and Seebeck coefficient. At the nanoscale, thermoelectric performances can be improved by increasing the number of interfaces and the frequency of diffuse phonon reflection. Ultimately, the phonon mean free path is reduced and consequently the thermal conductivity decreases [5].

Ag_2Te exists in 3 different phases: monoclinic α which undergoes at 418 K a phase transition into cubic β, this latter being stable between 418 and 1075 K and the phase γ between 1075 and 1233 K. Among these phases, monoclinic Ag_2Te has the best thermoelectric properties [6]. This compound behaves like a semiconductor with a narrow band gap [7] that can be adapted for low temperature thermoelectric applications [8].

The composition can be varied in order to control the nature of the charge carriers to obtain Te-rich structures (p-type) or Ag-rich structures (n-type) [9]. Ag_2Te has a high power factor due to high carrier mobility (Hall mobility μ_H = 6000 $cm^2/V.s$ at 300 K), a low lattice thermal conductivity (K = 1 W/m.K) and a high electric conductivity (σ = 25 S/m at 300 K) [7]. Park et al. have measured reduced thermal conductivity (K = 0.35 W/m.K) for nanorods by comparison with bulk values [10]. Hence this work will focus on the synthesis of nanostructures of Ag_2Te.

Ag_2Te nanostructures can be obtained by different methods: solvothermal [4], [9], [11]–[15] or hydrothermal reduction [16]–[21], by electrodeposition [2], [22], by high intensity ultrasonic irradiation in organic solvents [23], by vapor transport technique [5], [24], or spark plasma sintering [4]. Common synthesis methods are hydrothermal and solvothermal routes, that can be divided in two main approaches:

* Corresponding author.
Email address: karen.al-hokayem@univ-lorraine.fr

- A single step synthesis [4], [12], [16]–[18], [21] consists in mixing Te(IV) and Ag(I) as metallic precursors in the presence of a reducing agent (ethylene glycol (EG), ascorbic acid, hydrazine, KBH_4...). The precursors of Te are usually TeO_2, $TeCl_4$ and Na_2TeO_3, dissolved in an aqueous solution [17] or in organic solvent such as EG which can act also as a reducing agent [18]. Using these methods, the reaction kinetics is slow and takes between 24 and 48 hours. In addition, it is difficult to avoid impurities such as silver particles and Te rich nanostructures. Indeed, the reaction is very sensitive to pH that must be adjusted to basic values to avoid the formation of Ag_7Te_4 and Ag particles on the surface of Ag_2Te nanostructures [12]. The presence of Ag(0) particles is due to an insufficient relative quantity of reduced Te(0), leading to the reduction of silver cations into their metallic counterpart [16]. Sometimes complexing agents like disodium salt of ethylenediaminetetraacetic acid Na_2(EDTA) [12] or 3-mercaptopropionic acid MPA [21] are added to control kinetics and to avoid the apparition of silver impurities. Finally, another disadvantage of the single step synthesis is the difficulty to control the size and the crystallinity of the resulting nanostructures.

- A two-step synthesis [9], [11], [13]–[15], [19], [20], can be alternatively conducted, where either Te or Ag (nanostructures or films) is first obtained and further converted into Ag_2Te by a redox reaction [11] whose mechanism is not well known until now. This two steps method allows preserving the crystallinity and the purity of the Te nanorods. Moreover, it prevents the formation of Ag particles on the surface of Ag_2Te nanostructures and of by-products ($Ag_{4.5}Te_3$, Ag_5Te_3, Ag_7Te_4…) [14]. Different parameters influence the composition, the crystalline quality and the morphology of Ag_2Te like bath temperature, time of reaction, Ag(I):Te molar ratio, addition of a Reducing Agent (RA) and the RA:Ag(I) molar ratio. In most cases EG is used, playing both roles of solvent and Ag(I) reducing agent and avoids the formation of by-products [20]. Only Jao et al. [11] and Samal et al. [19] synthesized Ag_2Te nanowires without any addition of a reducing agent. In this case, Te acts both as template and Ag(I) reducing agent but polycrystalline structures are obtained even if the initial Te nanowires are single crystalline [19].

In this work, we present a two-step synthesis route of single crystalline Ag_2Te nanorods of high purity. The synthesis occurs in mild conditions: room temperature, atmospheric pressure and without any addition of toxic solvents, reducing agents, surfactants or complexing agents. One-dimensional hexagonal single crystalline Te nanorods are first obtained by electrodeposition in an ionic liquid medium, taking advantage of its templating properties. Te nanorods are then transformed into pure single crystalline and defect free α Ag_2Te nanorods (monoclinic phase, hessite) via a combination of cementation and topotactic reactions, with a slight increase in diameter. The influence of reaction time and Ag(I):Te molar ratio on the transformation of Te in Ag_2Te is presented.

2. Experimental

2.1. Chemicals

$TeCl_4$ (99%, Alfa Aesar) was used as precursor of Te(IV), whereas $AgNO_3$ (analytical reagent, VWR) was used as precursor of Ag(I). 1-ethyl-1-octyl-piperidinium bromide (EOPipBr) and 1-ethyl-1-octyl-piperidinium bis(trifluoromethylsulfonyl)imide (EOPipTFSI) ionic liquids (ILs) were synthesized as described by Traore et al. [25] and characterized by nuclear magnetic resonance analysis (Bruker Avance 400 MHz) then stored in a glove box to minimize water/oxygen contents (Mbraun Labstar, O_2/H_2O levels < 1 ppm).

2.2. Synthesis of Ag_2Te nanostructures

2.2.1. First step

The synthesis of Te nanorods was performed inside a glovebox (Mbraun Labstar, O_2/H_2O levels < 1 ppm). The electrochemical deposition of Te nanostructures was achieved at 100 °C in a mix of EOPipTFSI:EOPipBr 95:5 mol% ionic liquids containing 5 mM $TeCl_4$. Bromide anion plays the role of complexing agent for the Te(IV) salt, improving its solubility in the IL [26]. The working electrode and the counter electrode were 300 nm thick platinum-coated glass slides (25 x 10 x 1 mm) purchased from Applications Couches Minces (ACM). A Pt wire was used as a pseudo-

* Corresponding author.
Email address: karen.al-hokayem@univ-lorraine.fr

reference electrode. The deposition surfaces were equal to 0.5 cm². All the electrodes were immerged in a 5 mL electrolyte solution. Te nanostructures were obtained by potentiostatic deposition for a fixed charge density Q (C/cm²).

Prior to Te electrodeposition, platinum-coated glass slides were cleaned by sonication in acetone (2 x 20 minutes) and then in ethanol (20 minutes). The air-dried resulting surfaces were then free of organic contamination. Then the surface of the Pt working electrode undergoes an electrochemical activation by cyclic voltammetry: 50 cycles were performed in 25 mL of 0.5 M H_2SO_4 between -0.17 V (potential of reductive adsorption of protons) and 1.2 V (potential of formation of Pt oxides). This allows a crystal reconstruction of Pt surface by repeated adsorption and desorption of oxygen and hydrogen atoms [27].

2.2.2. Second step

The second step concerns the conversion of Te to Ag_2Te nanorods by chemical cementation. The Pt substrate on which the Te nanorods were previously deposited was immerged in a 10 mL aqueous solution of $AgNO_3$ under stirring, at room temperature and without any addition of reducing agent. The cell was protected from the light with aluminum foil to avoid photochemical reduction of Ag(I). The Ag(I):Te molar ratio was varied, as well as the reaction time, in order to compare the resulting composition of nanorods.

2.3. Characterizations of the nanostructures

The morphology and chemical composition of Te and Ag_2Te nanostructured films were analyzed using a Scanning Electron Microscopy SEM Quanta FEG 650 microscope equipped with an Energy Dispersive X-ray (EDX) detector.

The Te deposition yield and the molar composition of Ag_2Te nanostructures were also evaluated by Inductively Coupled Plasma-Optical Emission Spectrometry (ICP-OES) using a Perkin Elmer Avio 200-OES after the mineralization of the deposits in 7 M nitric acid. Signals are collected through a cooled CCD-based detector, with simultaneous measurement of the background emission and a neon spectrum for active wavelength correction. The operating parameters were as follow: RF power: 1.5 kW; plasma gas flow 10 L min^{-1}, auxiliary gas flow 0.2 L min^{-1}, nebulizer gas flow 0.7 L min^{-1} and sample uptake rate 1.0 L min^{-1}. The following atomic line wavelengths were used in the measurements: Ag^{I} (328.068 nm) and Te^{I} (214.281 nm).

X-Ray Diffraction (XRD) analyses were carried out with a Bruker D8 Advance diffractometer using Cu Kα radiation (λ = 1.5406 Å) at 40 kV and 40 mA. The samples were scanned in the 2θ range from 10° to 70° but only the reduced range 20° to 60° was analyzed, where all the main peaks of the Te-based phases were expected. The crystallographic phases were analyzed on the basis of the JCPDS databases with the EVA 5 software.

The mean diameter and length of Te and Ag_2Te nanorods were measured on images of individuals nanorods acquired by a Philips CM200 Transmission Electron Microscope (TEM) operating at an accelerating voltage of 160 kV.

High Resolution-Transmission Electron Microscopy (HR-TEM) analysis was performed on a JEM - ARM 200F cold Field Emission Gun TEM/Scanning TEM

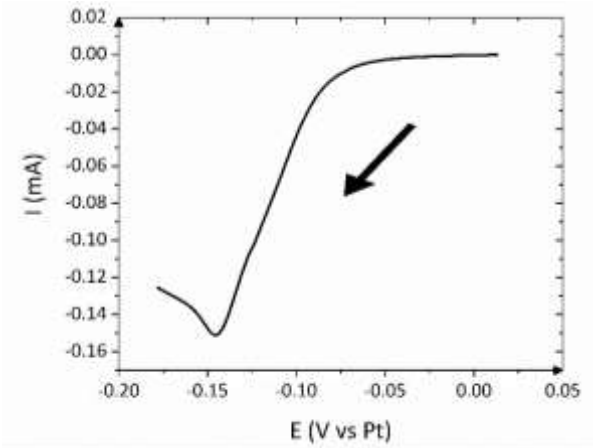

Fig. 1: Typical linear sweep voltammogram of the reduction of Te(IV) to Te(0) in EOPipTFSI:EOPipBr 95:5 (mol%). [$TeCl_4$] = 5 mM. Pt-coated glass slide substrate. T = 100 °C, scan rate 5 mV s^{-1}.

* Corresponding author.
Email address: karen.al-hokayem@univ-lorraine.fr

(cFEG TEM/STEM) operating at 200 kV and equipped with a spherical aberration (Cs) probe and image correctors (point resolution 0.12 nm in TEM mode and 0.078 nm in STEM mode). The growth direction of the nanostructures was determined by imaging and Selected Area Electron Diffraction (SAED). The chemical composition of individual nanostructures was analyzed by EDX (mapping and line profile).

3. Results and discussion

3.1. Synthesis of Te nanorods

The first step of the process allows to obtain a thin film of self-standing Te nanorods by applying a fixed cathodic potential. This result is a consequence of the anisotropic crystalline structure of Te [28], the limitation of electrochemical growth by mass transport [26] and the templating properties of the ionic liquid [29]. The value of the applied potential is defined by the position of the peak observed in a preliminary cathodic linear sweep voltammetry (Fig. 1). This cathodic peak corresponds to the reduction of Te(IV) to Te(0) according to the following chemical equation:

$$TeX_6^{2-} + 4e^- \rightarrow Te + 6X^-$$

where X^- may be attributed to Cl^- or Br^- anions [26]. This procedure was derived from the works of J.Szymczak et al. [30] and L.Thiebaud et al. [26] and adapted to obtain reduced and uniform dimensions (Fig. 2). It appears that the diameter and length of the 1D Te nanostructures are directly related to the coulometric charge. The tellurium concentration and the bromide content have a lesser impact. Thus, with [Te(IV)] = 5 mM and [Br^-] = 0.25 mM (5% mol), the smallest nanorods were obtained by applying a charge density Q of 0.1 C/cm². The mean diameter is of 60 ± 13 nm and length of 191 ± 41 nm as shown in Fig. 3. The mass per unit area of electrodeposited Te nanorods, measured by ICP-OES, is equal to 30 µg/cm², corresponding to a faradic yield of 90%.

SAED and HR-TEM results (Fig. 4) show that the electrodeposited Te nanorods are single crystalline, with an hexagonal lattice and a preferential orientation along the [001] direction (JCPDS n° 00-036-1452). This observation is in perfect agreement with our previous published results for Te nanostructures with greater dimensions [26].

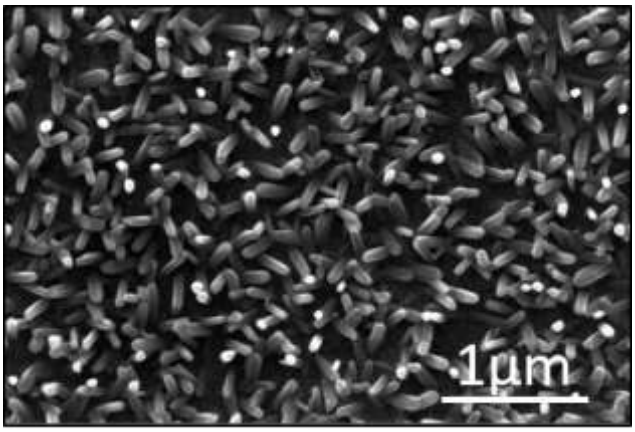

Fig. 2: SEM image of Te nanorods electrodeposited at C_1 peak potential in EOPipTFSI:EOPipBr 95:5 (mol%). [$TeCl_4$] = 5 mM. T = 100 °C, Q = 0.1 C/cm², Pt-coated glass slide.

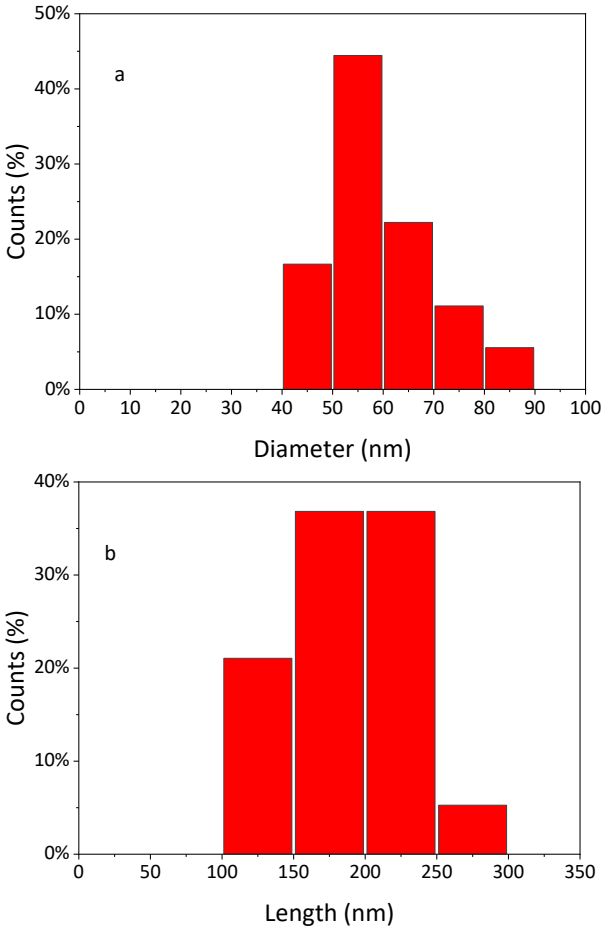

Fig. 3: a) Diameter and b) Length of Te nanorods deposited at C_1 peak potential in EOPipTFSI:EOPipBr 95:5 (mol%). [$TeCl_4$] = 5 mM. T = 100 °C, Q = 0.1 C/cm² (number of analyzed nanowires n = 18).

3.2. Synthesis of Ag_2Te nanorods

* Corresponding author.
Email address: karen.al-hokayem@univ-lorraine.fr

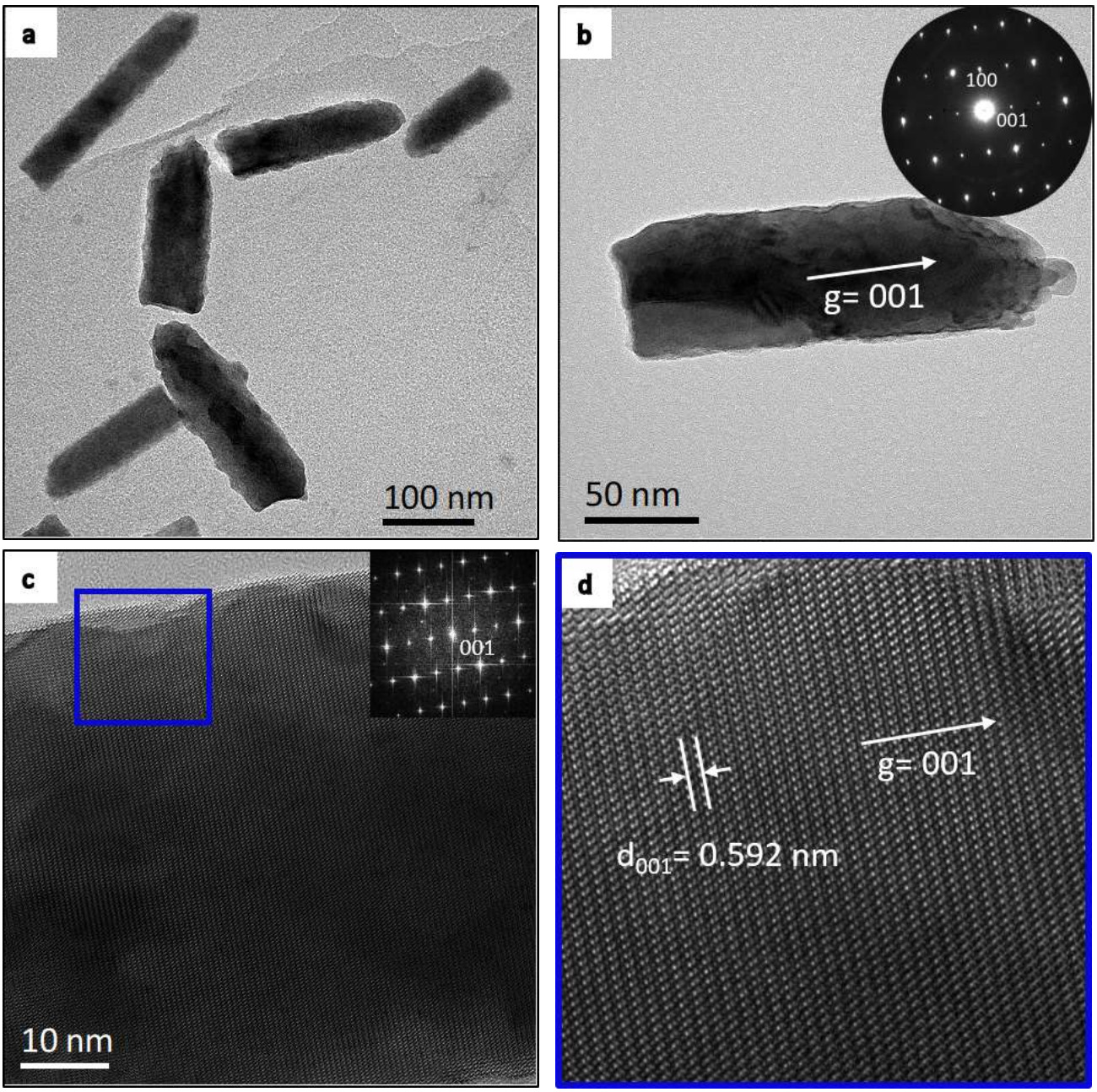

Fig. 4: TEM characterization of Te nanorods: a) TEM image of a Te nanorods group, b) TEM micrograph and corresponding SAED pattern indexed to the tellurium phase along the [010] zone axis (SG: $P3_121$), c) HRTEM micrograph with Fast Fourier Transform (FFT) and d) Zoom on the blue square of Te crystallographic structure along the [010] zone axis (JCPDS n° 00-036-1452).

Synthesized Te nanostructures were then used to prepare Ag_2Te nanorods by chemical reaction with silver cations Ag^+ (Ag(I)) in aqueous solution. The influence of nAg(I)/nTe ratio on the chemical composition of the deposit was first studied by ICP-OES for a 24h immersion time. As shown in Fig. 5, the silver content in the nanostructures progressively increases with the nAg(I)/nTe ratio in the bath, until a value close to Ag_2Te for a ratio ≥ 2. Similarly, nearly stoichiometric $Ag_{2.04}Te$ nanowires were obtained by Yang et al. for nAg(I)/nTe = 3 but in presence of a reducing agent and the nanowires they obtained were polycrystalline [9]. Kim et al. also observed that a large excess of Ag (value not specified in their work) is needed to reach $Ag_{2.13}Te$ in a two-step synthesis in the presence of EG [20]. In our work, the resulting nanostructured film appear to be homogeneous on the surface as shown by the SEM image (Fig. 6a). Moreover the presence of Ag and Te is confirmed by the EDX spectrum (Fig. 6b) and is uniformly distributed along the nanostructures (Fig. 6c). When a large excess of Ag(I) is used (nAg(I)/nTe = 772), SEM

* Corresponding author.
Email address: karen.al-hokayem@univ-lorraine.fr

analysis reveals the presence of large Ag_2Te 2D cross braces of micrometer size on the surface of the nanostructured film (Fig. 7). These large grains due to overgrowth appear after 30 minutes of immersion.

The influence of immersion time was then studied for nAg(I)/nTe ratio = 2, which leads to highly crystalline nanorods and homogeneous films of nanostructures. The crystallographic transition from hexagonal Te to monoclinic hessite α-Ag_2Te was followed by XRD analysis according to the following procedure: after a reaction time of 30 minutes, the Te sample was removed from Ag(I) solution, rinsed, analyzed by XRD and then immersed again in the same solution. This experimental sequence was repeated for 1h, 2h, 4h and 6h reaction time. Corresponding diffractograms are given in Fig. 8. Before reaction takes place, two

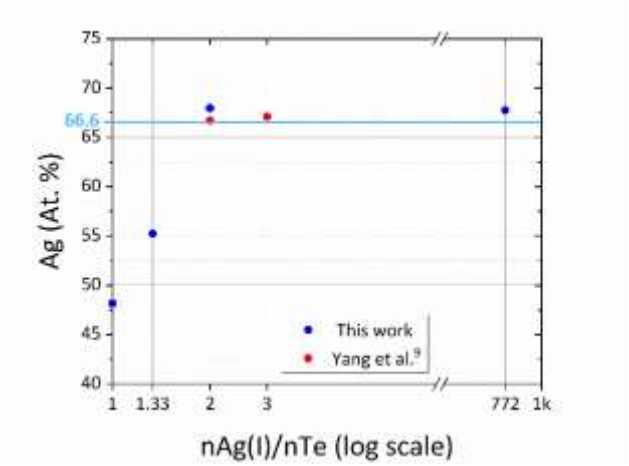

Fig. 5: Influence of nAg(I)/Te molar ratio in the bath on the final composition of Ag_2Te nanowires: ICP-OES analysis after chemical dissolution of the deposits.

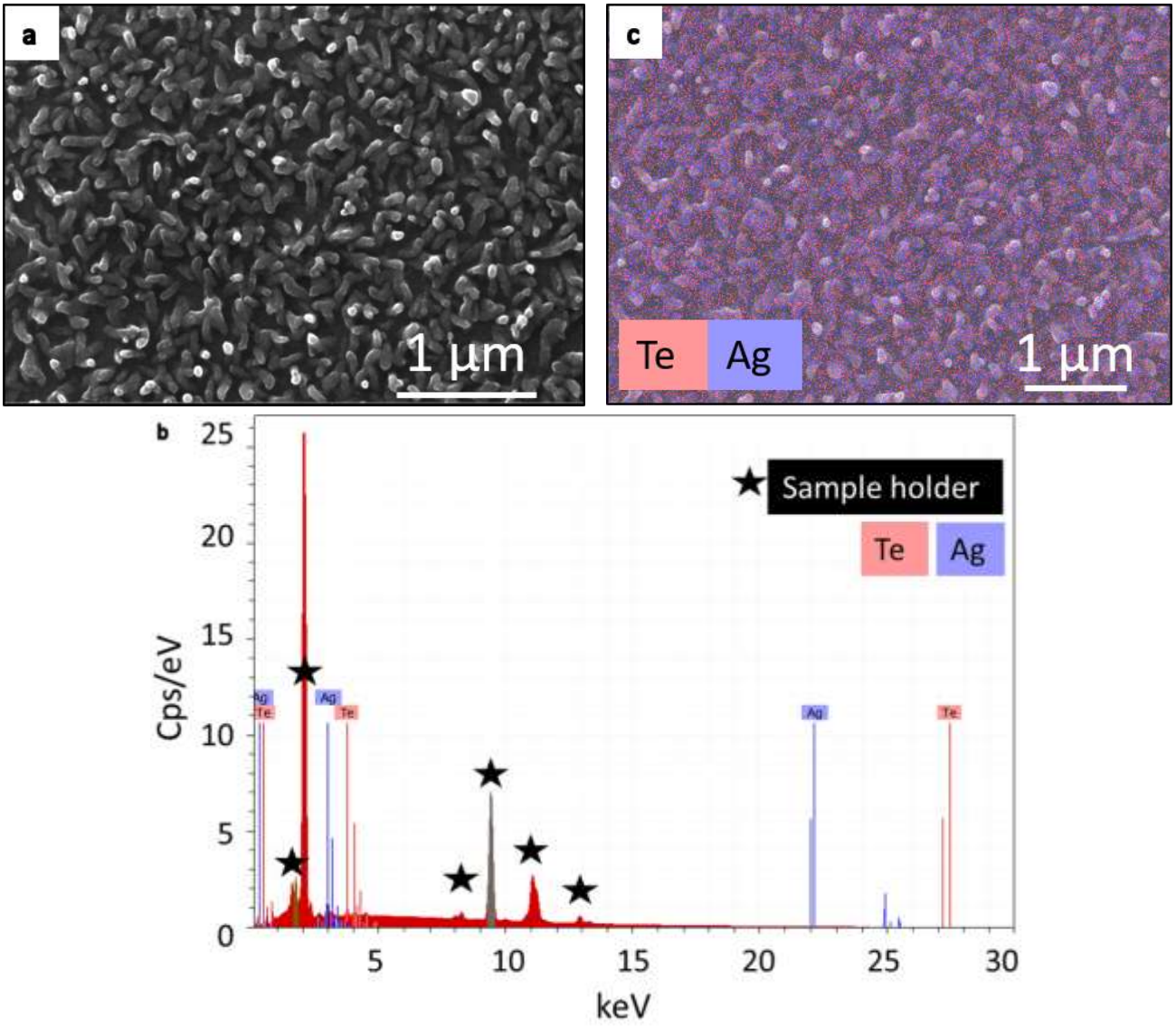

Fig. 6: SEM characterization of Ag_2Te nanorods film after 24h immersion prepared with nAg(I)/nTe = 2: a) SEM image, b) EDX spectrum, c) EDX mapping.

* Corresponding author.
Email address: karen.al-hokayem@univ-lorraine.fr

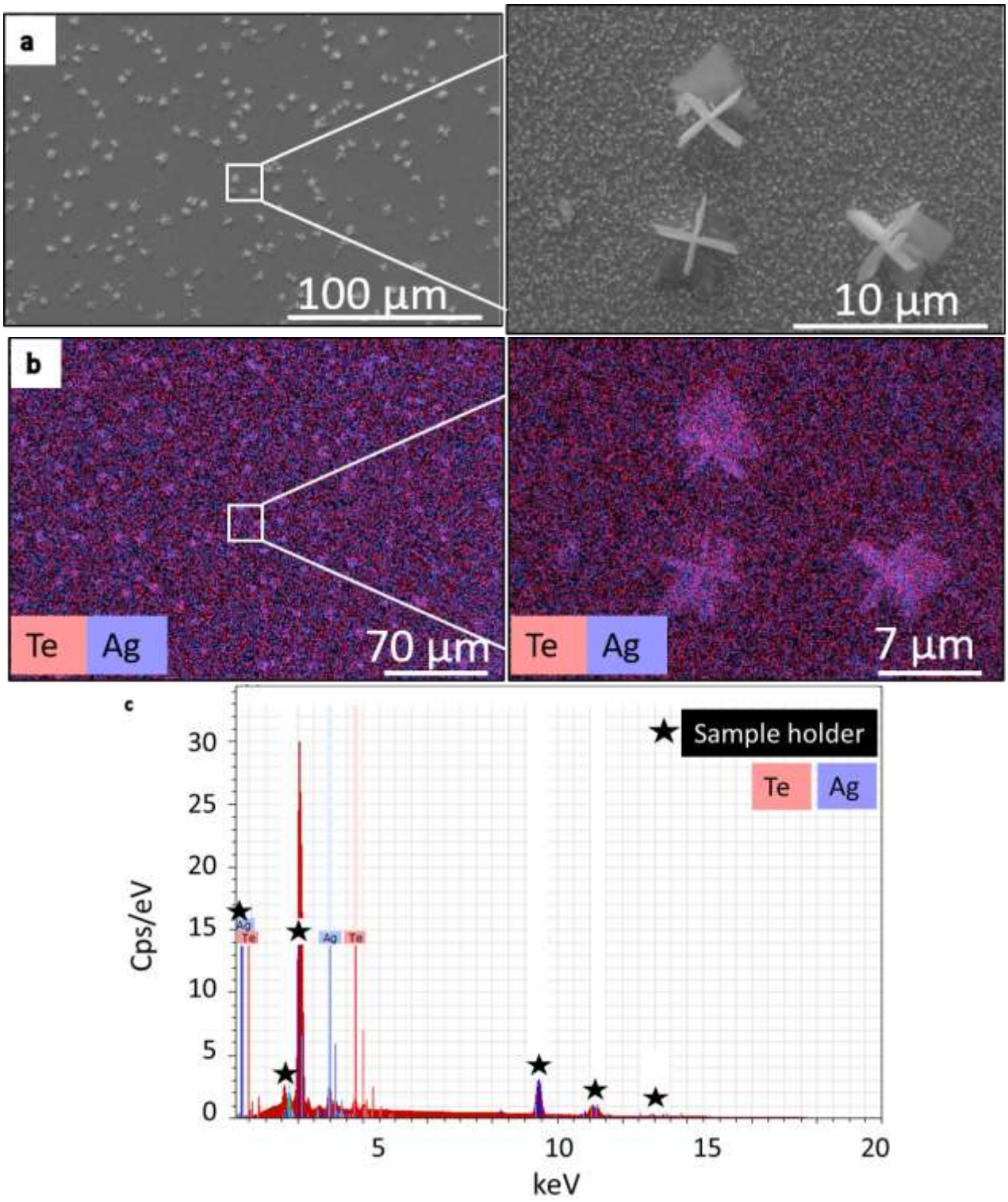

Fig. 7: SEM characterization of Ag_2Te nanorods film after 24h immersion prepared with nAg(I)/nTe = 772: a) SEM image, b) EDX mapping, c) EDX spectrum.

peak at 27.7° and 57.07° attributed to hexagonal Te are observed. These peaks decrease as reaction time increases. Thus, the one at 27.7° disappears completely after a reaction time of 4h, while the peak at 57.07° disappears after 2h. In parallel, two small peaks at 29.9° and 31.05° that are attributed to hessite Ag_2Te appear after 4h of immersion and increase with reaction time (Fig. 8). These peaks are of low intensity despite the crystallinity of the nanorods confirmed by SAED. The Pt substrate peak masks the angular domain 2theta 35°-47°. After 6h immersion time, ICP-OES analysis of the sample

* Corresponding author.
Email address: karen.al-hokayem@univ-lorraine.fr

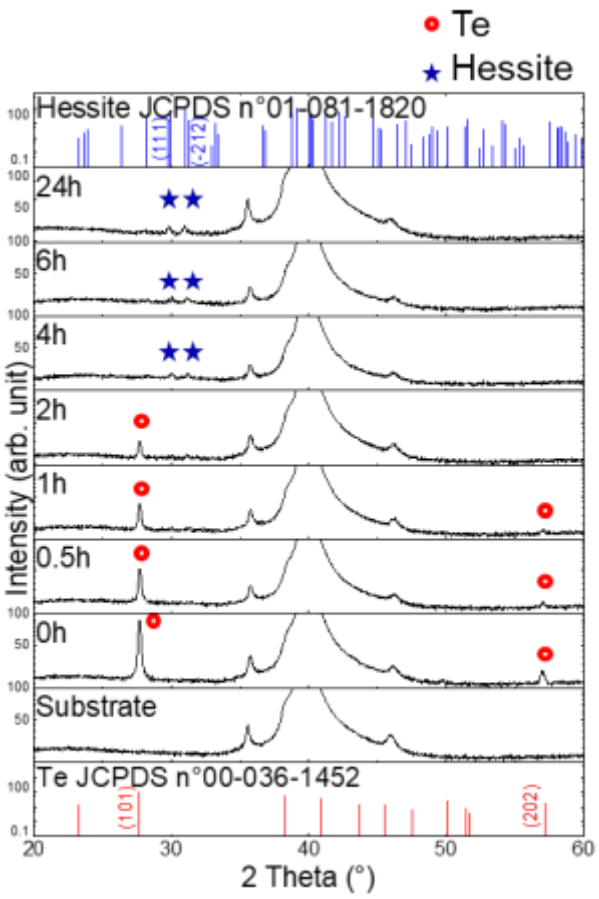

Fig. 8: XRD characterization: Crystallographic transition from hexagonal Te to monoclinic hessite Ag_2Te with nAg(I)/nTe = 2.

reveals an Ag:Te mean molar ratio of nanorods equal to 2.1 corresponding to $Ag_{2.1}Te$. This ratio does not change whenever the immersion time is further increased.

However, HR-TEM analysis after a reaction time of 6h reveals the presence of an intermediate compound, the hexagonal stützite phase ($Ag_{1.5}Te$ JCPDS n° 04-008-4552), with [001] growth direction (Fig. 9). EDX analyses of individual nanostructures give $Ag_{1.8}Te$ (Fig. 10), which agrees with the deficit of silver of the stützite phase. However, this ratio is lower than the mean ratio measured by ICP-OES ($Ag_{2.1}Te$), suggesting that the transformation is not fully completed on the whole surface of the sample after 6h immersion. The composition and the morphology of these stützite nanorods appear uniform (Fig. 10 and Fig. 11). Slight curvatures are observed (Fig. 9). After 24h reaction time, the complete transformation of hexagonal Te into highly pure single crystalline monoclinic α- Ag_2Te (hessite Ag_2Te JCPDS n° 01-081-1820), more stable than the stützite phase, is achieved, as confirmed by

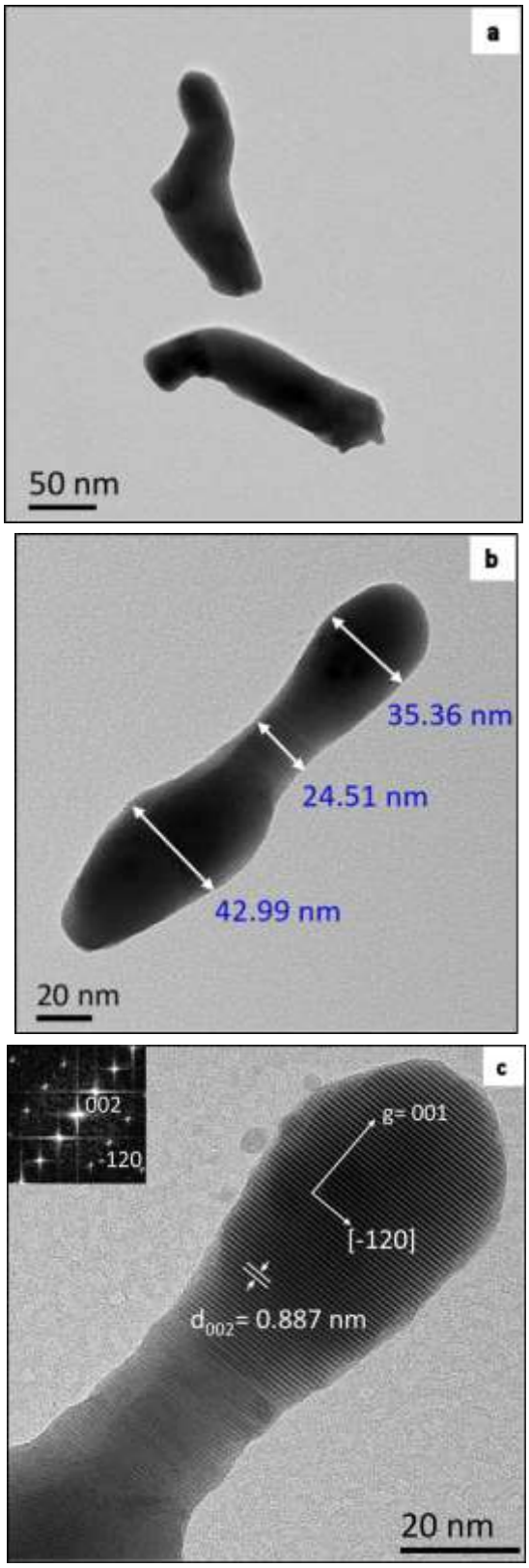

Fig. 9: TEM characterization of stutzite nanorods after 6h immersion, prepared with nAg(I)/nTe = 2: a) TEM image of a stutzite slightly curved nanorods group, b) TEM image of diameter-enhanced stutzite nanorod, c) corresponding HRTEM micrograph and Fast Fourier Transform (FFT) of stutzite crystallographic structure along the [210] zone axis (SG: P-62m) (JCPDS n° 04-008-4552).

* Corresponding author.
Email address: karen.al-hokayem@univ-lorraine.fr

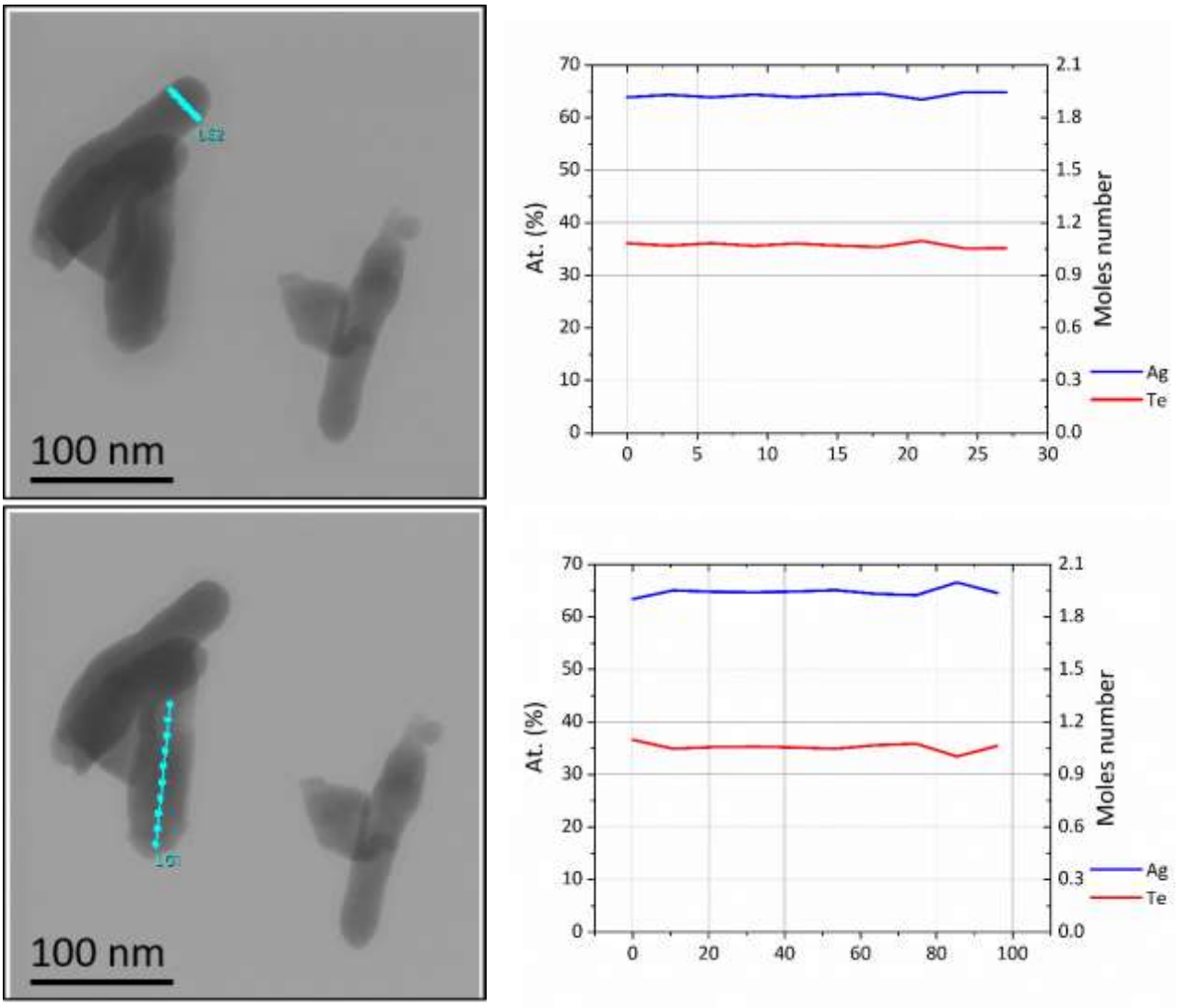

Fig. 10: Line profil analysis of stutzite nanorods after 6h immersion prepared with nAg(I)/nTe = 2.

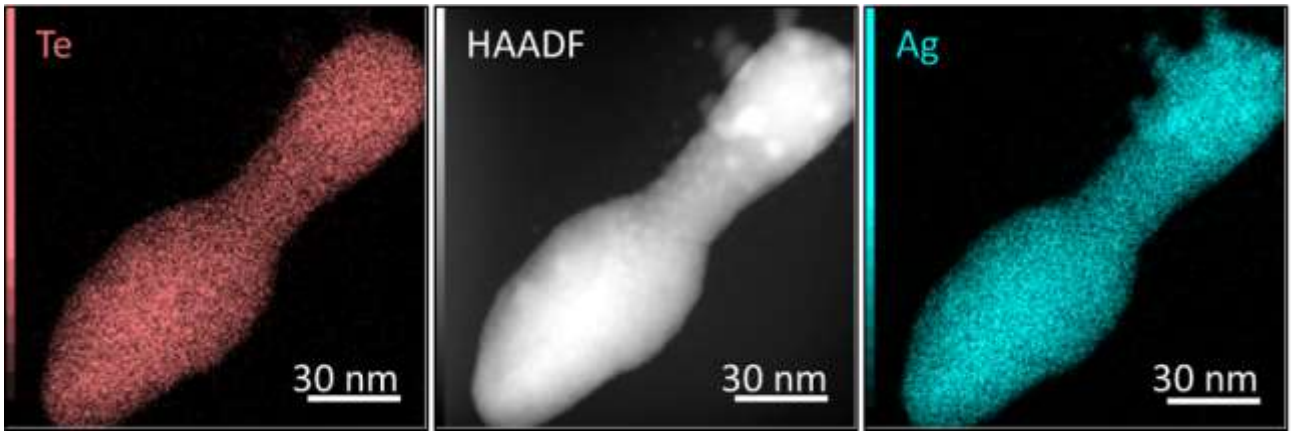

Fig. 11: Elemental X maps of a stutzite nanorod after 6h immersion prepared with nAg(I)/nTe = 2.

SAED analysis (Fig. 12). The transformation from Te to Ag_2Te is thermodynamically favorable [14]. A slight increase in diameter of about 5 to 30 % (~ 3-20 nm) is observed compared to initial Te nanorods (Fig. 13) along with a curvature of some nanorods (Fig. 12). By adding EG as reducing agent, the volume expansion was reported to be greater and can reach 2 times the initial nanostructures in the literature data. When the volume expansion becomes considerable, Te nanowires tend to bend and break into shorter

* Corresponding author.
Email address: karen.al-hokayem@univ-lorraine.fr

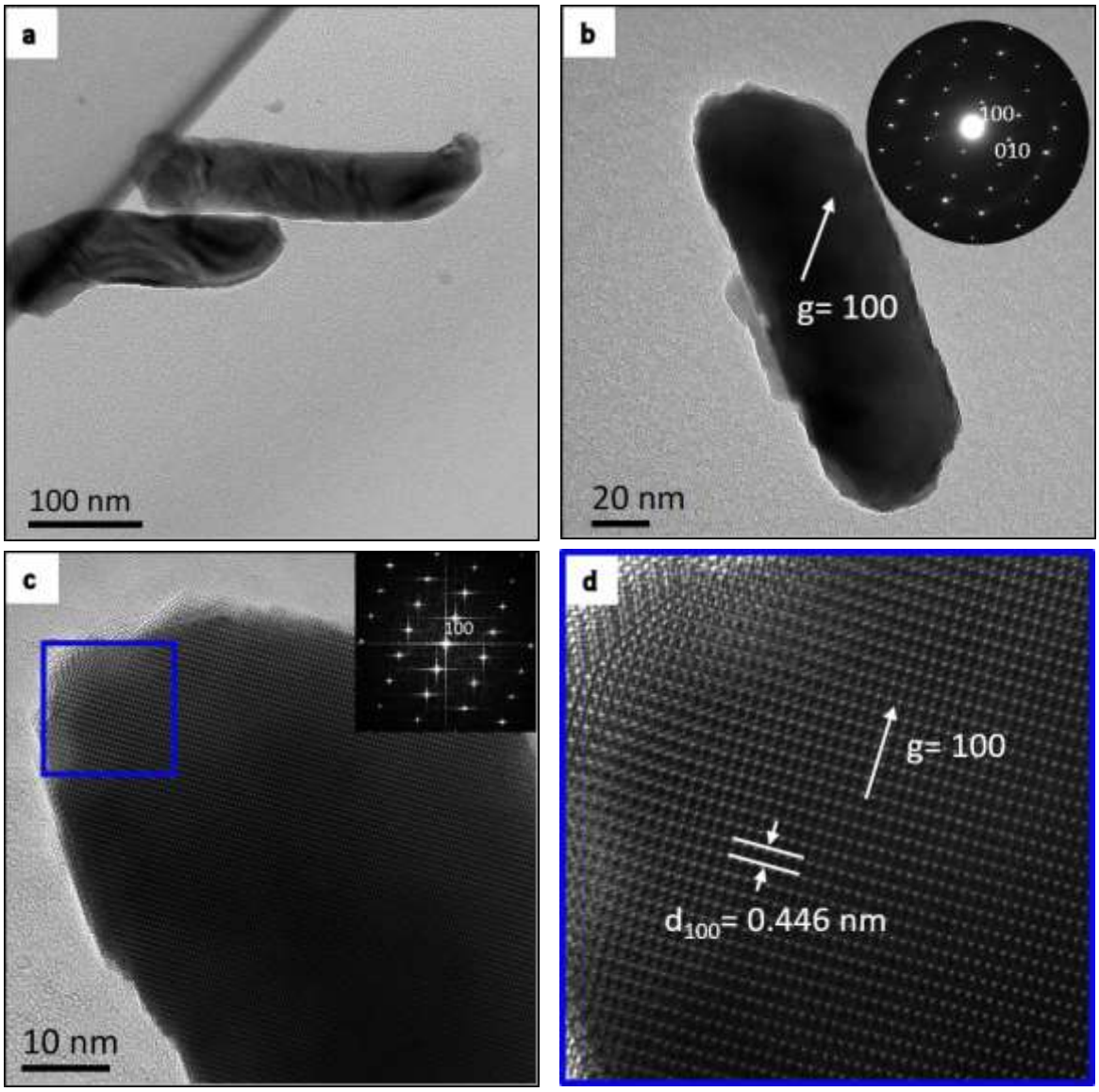

Fig. 12: TEM characterization of hessite nanorods after 24h immersion prepared with nAg(I)/nTe = 2: a) TEM image of a Ag_2Te nanorods group, b) TEM micrograph and corresponding SAED pattern indexed to the hessite phase along the [001] zone axis (SG: $P12_1/C1$), c) HRTEM micrograph with Fast Fourier Transform (FFT) and d) Zoom on the blue square of Ag_2Te crystallographic structure along the [001] zone axis (JCPDS n° 01-081-1820).

nanowires but the single crystallinity is conserved [14]. In this work, the volume increase is avoided by sacrificing a part of the Te as reducing agent. Indeed, chemical analysis by ICP-OES revealed the presence of tellurium in the bath after the cementation process. This result is a consequence of the partial oxidation of the tellurium nanostructures in the form of dissolved tellurium (IV), avoiding the volume increase. The nanorods always remain single crystalline as a sign of the homogeneous transformation on the surface of the nanorods. The same kinetic study was performed in large excess of Ag(I) (nAg(I)/nTe = 772). Surprisingly, the kinetics of Te conversion to Ag_2Te is not faster and even slightly slowed down according to XRD results (Fig. 14): when nAg(I)/nTe = 2, the peak of Te at 27.7° disappears after a reaction time of 8h instead of 4h. The peak at 57.07° disappears after 4h instead of 2h.

From these observations, the following mechanism can be proposed. The transformation of Te into Ag_2Te occurs in two steps: a transformation by chemical cementation, during which Ag(I) is reduced by Te (reaction (1)), followed by a topotactic transformation implying Ag atoms entering the Te structure (reaction (2)) [14], [20].

$$4Ag(I) + Te(0) \rightarrow 4Ag(0) + Te(IV) \qquad (1)$$

* Corresponding author.
Email address: karen.al-hokayem@univ-lorraine.fr

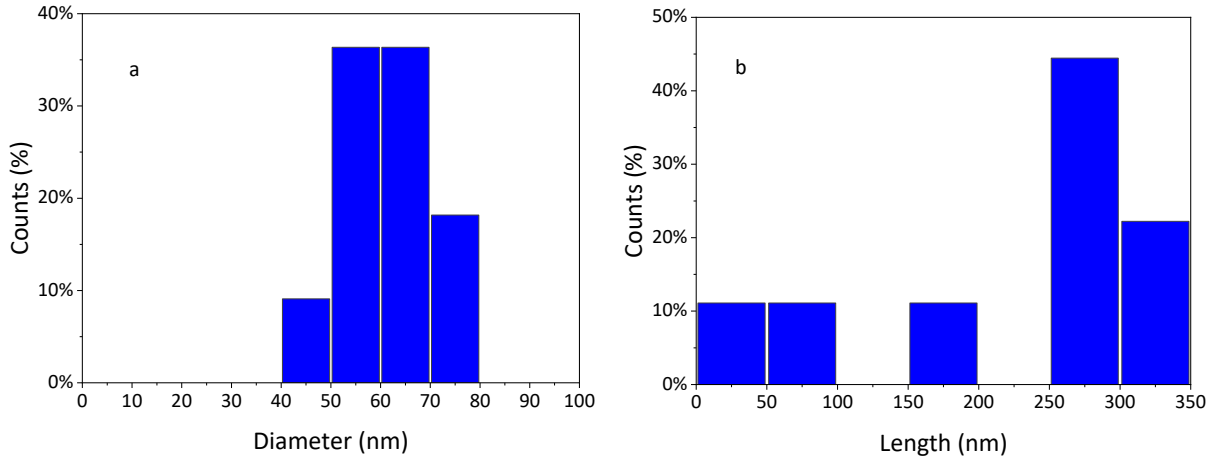

Fig. 13: a) Mean diameter and b) Length of hessite nanorods after 24h immersion prepared with nAg(I)/nTe = 2 (number of analyzed nanowires n = 9).

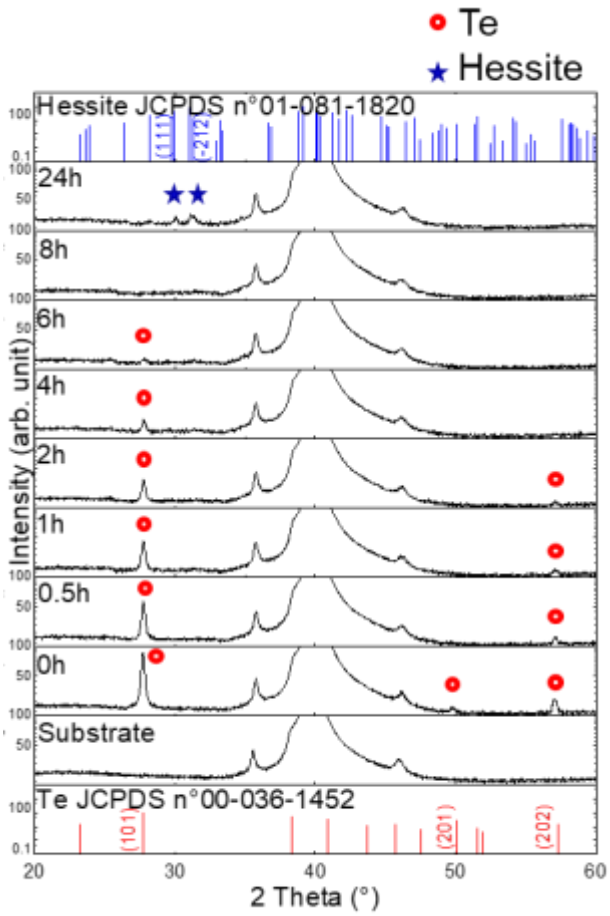

Fig. 14: XRD characterization: Crystallographic transition from hexagonal Te to monoclinic hessite Ag_2Te with nAg(I)/nTe = 772.

$$4Ag(0) + 2Te(0) \rightarrow 2Ag_2Te \qquad (2)$$

The global reaction (reaction (3)) can be written as:

$$4Ag(I) + 3Te(0) \rightarrow 2Ag_2Te + Te(IV) \qquad (3)$$

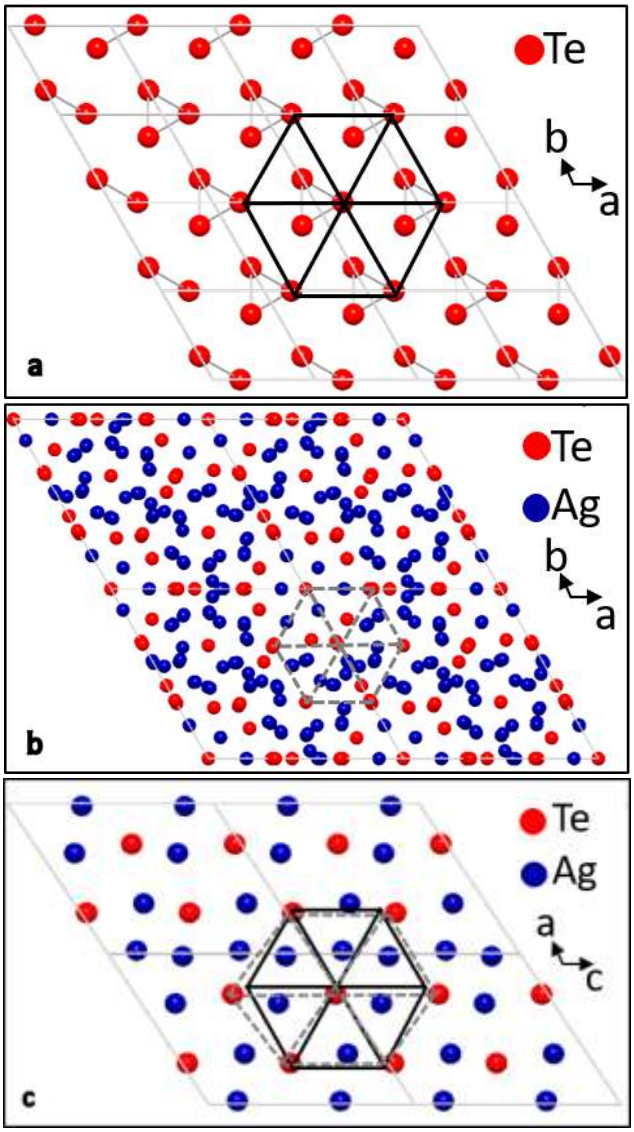

Fig. 15: Crystalline structure of a) Hexagonal Te; b) Hexagonal stutzite; c) Monoclinic hessite.

* Corresponding author.
Email address: karen.al-hokayem@univ-lorraine.fr

From our observations, only a slight excess of Ag in the Ag_2Te nanostructures is observed even if the molar ratio of precursors (n(Ag(I))/n(Te)) is superior to the stoichiometric ratio 4/3 according to the equation (3).

A time progressive incorporation of silver occurs in the tellurium hexagonal crystalline structure. After 6h, Te-rich Ag_2Te nanorods are obtained with the stützite phase (hexagonal symmetry, P-62m). Then a phase transition occurs together with an increase of Ag content in the nanostructures. Finally, the synthesis is considered as complete after a reaction of 24h, where the stoichiometry reaches Ag_2Te with a slight excess of Ag and the nanorods are crystallized according the hessite phase (monoclinic phase, $P12_1/C1$). The corresponding crystallographic cells of the 3 successive phases are displayed in the Fig. 15, highlighting that the hexagonal symmetry of Te atoms is kept whatever the phases. This observation of the final phase is similar to the transformation of trigonal Se nanowires into orthorhombic Ag_2Se nanowires, which is justified by the topotactic lattice matching between the both phases. Similar transformation from hexagonal Te to Ag_2Te was also observed and discussed by Moon at al. in terms of volume changes of the cell [14]. In our work, the partial consumption of tellurium can explain the only slight increase in diameter (5-30%) compared to the 100% volume expansion observed in literature by adding a reducing agent [14]. The final dimensions of the nanostructures being close to initial ones suggest that no breakage of the nanorods due to stress release occurs during the transformation.

4. Conclusions

The two-step way used in this work allows synthesizing highly pure single crystalline monoclinic Ag_2Te nanorods by chemical cementation reaction, using Te nanorods both as template and reducing agent. The hexagonal single crystalline self-standing tellurium nanorods of 60 ± 13 nm in diameter and less than 200 nm long were firstly electrodeposited in an ionic liquid medium. The further cementation reaction consists in the reduction of Ag(I) to Ag(0) by Te on the surface of the nanorods, followed by the incorporation of the Ag atoms in the hexagonal lattice of Te. A phase transition occurs as the stoichiometry reaches targeted Ag_2Te. The mechanism of this reaction was experimentally highlighted for the first time, thanks to the observation of an intermediate stützite phase. Single crystalline hessite Ag_2Te nanorods are finally obtained with uniform size and chemical composition. This two-step synthesis, performed in mild conditions (room temperature, atmospheric pressure) and without any addition of toxic solvents, reducing agents or surfactants, appears to be attractive for the dedicated synthesis of high quality silver telluride nanostructures.

Author Contributions

Conceptualization K.A., S.L. and N.S
Methodology K.A., S.M. and J.G.
Validation K.A., S.L. and N.S
Writing - original draft preparation K.A.
Writing - review S.L. and N.S
Editing K.A.

Conflicts of interest

There are no conflicts to declare.

Acknowledgements

This work was supported by the Grand Est Region under the Nanohyb project.

Sebastien DILIBERTO (from Université de Lorraine, CNRS, IJL, F-57000 Metz, France) and Sylvie MIGOT (from Université de Lorraine, CNRS, IJL, F-54000 Nancy, France) are acknowledged for their technical support.

References

[1] S. K. Batabyal and J. J. Vittal, "Axial-junction nanowires of Ag2Te-Ag as a memory element," *Chemistry of Materials*, vol. 20, no. 18, pp. 5845–5850, 2008, doi: 10.1021/cm801388w.

[2] V. B. Prabhune and V. J. Fulari, "Measurement of properties of silver telluride thin films using holography," *Optics Communications*, vol. 282, no. 11, pp. 2118–2122, 2009, doi: 10.1016/j.optcom.2009.02.029.

[3] M. Lee, T. F. Rosenbaum, M. L. Saboungi, M. L. Saboungi, and H. S. Schnyders, "Band-gap tuning and linear

* Corresponding author.
Email address: karen.al-hokayem@univ-lorraine.fr

magnetoresistance in the silver chalcogenides," *Physical Review Letters*, vol. 88, no. 6, pp. 66602/1-66602/4, 2002, doi: 10.1103/PhysRevLett.88.066602.

[4] Y. Chang, J. Guo, Y. Q. Tang, Y. X. Zhang, J. Feng, and Z. H. Ge, "Facile synthesis of Ag2Te nanowires and thermoelectric properties of Ag2Te polycrystals sintered by spark plasma sintering," *CrystEngComm*, vol. 21, no. 11, pp. 1718–1727, 2019, doi: 10.1039/c8ce01863d.

[5] S. Lee, H. S. Shin, J. Y. Song, and M. H. Jung, "Thermoelectric Properties of a Single Crystalline Ag2Te Nanowire," *Journal of Nanomaterials*, vol. 2017, pp. 14–19, 2017, doi: 10.1155/2017/4308968.

[6] M. Fujikane, K. Kurosaki, H. Muta, and S. Yamanaka, "Thermoelectric properties of α- And β-Ag2Te," *Journal of Alloys and Compounds*, vol. 393, no. 1–2, pp. 299–301, 2005, doi: 10.1016/j.jallcom.2004.10.002.

[7] Y. Pei, N. A. Heinz, and G. J. Snyder, "Alloying to increase the band gap for improving thermoelectric properties of Ag2Te," *Journal of Materials Chemistry*, vol. 21, no. 45, pp. 18256–18260, 2011, doi: 10.1039/c1jm13888j.

[8] Y. Wang *et al.*, "Design guidelines for chalcogenide-based flexible thermoelectric materials," *Materials Advances*, vol. 2, no. 8, pp. 2584–2593, 2021, doi: 10.1039/d0ma01018a.

[9] H. Yang *et al.*, "Composition modulation of Ag2Te nanowires for tunable electrical and thermal properties," *Nano Letters*, vol. 14, no. 9, pp. 5398–5404, 2014, doi: 10.1021/nl502551c.

[10] D. Park, H. Ju, T. Oh, and J. Kim, "Facile fabrication of one-dimensional Te/Cu2Te nanorod composites with improved thermoelectric power factor and low thermal conductivity," *Scientific Reports*, vol. 8, no. 1, pp. 1–10, 2018, doi: 10.1038/s41598-018-35713-9.

[11] Y.-T. Jao, Y.-C. Li, Y. Xie, and Z.-H. Lin, "A Self-Powered Temperature Sensor Based on Silver Telluride Nanowires," *ECS Journal of Solid State Science and Technology*, vol. 6, no. 3, pp. N3055–N3057, 2017, doi: 10.1149/2.0101703jss.

[12] F. Xiao, G. Chen, Q. Wang, L. Wang, J. Pei, and N. Zhou, "Simple synthesis of ultra-long Ag2Te nanowires through solvothermal co-reduction method," *Journal of Solid State Chemistry*, vol. 183, no. 10, pp. 2382–2388, 2010, doi: 10.1016/j.jssc.2010.07.020.

[13] T. Sutch, J. M. Allred, and G. Szulczewski, " Electron conducting Ag 2 Te nanowire/polymer thermoelectric thin films ," *Journal of Vacuum Science & Technology A*, vol. 39, no. 2, p. 023401, 2021, doi: 10.1116/6.0000690.

[14] G. D. Moon, S. Ko, Y. Xia, and U. Jeong, "Chemical transformations in ultrathin chalcogenide nanowires," *ACS Nano*, vol. 4, no. 4, pp. 2307–2319, 2010, doi: 10.1021/nn9018575.

[15] E. K. Kim, D. Park, N. K. Shrestha, J. Chang, C. W. Yi, and S. H. Han, "A facile room temperature chemical transformation approach for binder-free thin film formation of Ag2Te and lithiation/delithiation chemistry of the film," *Dalton Transactions*, vol. 45, no. 43, pp. 17312–17318, 2016, doi: 10.1039/c6dt03038f.

[16] B. Zhong, X. Wang, Y. Bi, W. Kang, and L. Zhang, "Simple synthesis of crooked Ag2Te nanotubes and their photoelectrical properties," *New Journal of Chemistry*, vol. 45, no. 13, pp. 6100–6107, 2021, doi: 10.1039/d1nj00687h.

[17] N. Li, B. Zhao, S. Zhou, S. Lou, and Y. Wang, "Electrical properties of individual Ag 2Te nanowires synthesized by a facile hydrothermal

* Corresponding author.
Email address: karen.al-hokayem@univ-lorraine.fr

approach," *Materials Letters*, vol. 81, pp. 212–214, 2012, doi: 10.1016/j.matlet.2012.05.009.

[18] Y. Gao *et al.*, "Fabrication and Electrical Properties of Silver Telluride Nanowires," *Journal of Nanoscience and Nanotechnology*, vol. 20, no. 4, pp. 2628–2632, 2019, doi: 10.1166/jnn.2020.17330.

[19] A. K. Samal and T. Pradeep, "Room-temperature chemical synthesis of silver telluride nanowires," *Journal of Physical Chemistry C*, vol. 113, no. 31, pp. 13539–13544, 2009, doi: 10.1021/jp901953f.

[20] S. Kim *et al.*, "Synthesis and thermoelectric characterization of high density Ag2Te nanowire/PMMA nanocomposites," *Materials Chemistry and Physics*, vol. 190, pp. 187–193, 2017, doi: 10.1016/j.matchemphys.2017.01.019.

[21] Y. Y. Wang, K. F. Cai, J. L. Yin, Y. Du, and X. Yao, "One-pot fabrication and thermoelectric properties of Ag 2Te-polyaniline core-shell nanostructures," *Materials Chemistry and Physics*, vol. 133, no. 2–3, pp. 808–812, 2012, doi: 10.1016/j.matchemphys.2012.01.098.

[22] R. Chen, D. Xu, G. Guo, and L. Gui, "Silver telluride nanowires prepared by dc electrodeposition in porous anodic alumina templates," *Journal of Materials Chemistry*, vol. 12, no. 8, pp. 2435–2438, 2002, doi: 10.1039/b201007k.

[23] B. Li, Y. Xie, Y. Liu, J. Huang, and Y. Qian, "Sonochemical synthesis of nanocrystalline silver tellurides Ag2Te and Ag7Te4," *Journal of Solid State Chemistry*, vol. 158, no. 2, pp. 260–263, 2001, doi: 10.1006/jssc.2001.9103.

[24] K. Pillai, "Single Crystalline Highly Pure Long Ag2Te Nanowires for Thermoelectric Applications and its Structural Analysis.," *Journal of Materials Science: Materials in Electronics*, pp. 1–8, 2021, doi: 10.21203/rs.3.rs-220103/v1.

[25] Y. Traore, S. Legeai, S. Diliberto, G. Arrachart, S. Pellet-Rostaing, and M. Draye, "New insight into indium electrochemistry in a Tf2N-based room-temperature ionic liquid," *Electrochimica Acta*, vol. 58, no. 1, pp. 532–540, 2011, doi: 10.1016/j.electacta.2011.09.085.

[26] L. Thiebaud, S. Legeai, and N. Stein, "Tuning the morphology of Te one-dimensional nanostructures by template-free electrochemical deposition in an ionic liquid," *Electrochimica Acta*, vol. 197, pp. 300–306, 2016, doi: 10.1016/j.electacta.2015.12.084.

[27] D. Bengio, E. Mendes, S. Pellet-Rostaing, and P. Moisy, "Electrochemical behavior of platinum and gold electrodes in the aprotic ionic liquid N,N-Trimethylbutylammonium Bis(trifluoromethanesulfonyl)imide," *Journal of Electroanalytical Chemistry*, vol. 823, no. April, pp. 445–454, 2018, doi: 10.1016/j.jelechem.2018.06.034.

[28] L. Thiebaud, S. Legeai, J. Ghanbaja, and N. Stein, "Synthesis of Te-Bi core-shell nanowires by two-step electrodeposition in ionic liquids," *Electrochemistry Communications*, vol. 86, pp. 30–33, Jan. 2018, doi: 10.1016/j.elecom.2017.11.010.

[29] C. Janiak, "Ionic liquids for the synthesis and stabilization of metal nanoparticles," *Zeitschrift fur Naturforschung - Section B Journal of Chemical Sciences*, vol. 68, no. 10, pp. 1059–1089, 2013, doi: 10.5560/ZNB.2013-3140.

[30] J. Szymczak *et al.*, "Template-free electrodeposition of tellurium nanostructures in a room-temperature ionic liquid," *Electrochemistry Communications*, vol. 24, no. 1, pp. 57–60, 2012, doi: 10.1016/j.elecom.2012.08.013.

* Corresponding author.
Email address: karen.al-hokayem@univ-lorraine.fr